

**SHORT REPORT**

*Liver Metabolism*

# Mammary tumor development induces perturbation of liver glucose metabolism with inflammation and fibrosis

 Anouk Charlot,<sup>1,2</sup> Anthony Bringolf,<sup>2</sup>  Joris Mallard,<sup>2,3,4</sup> Amélie Jaulin,<sup>5</sup> Emilie Crouchet,<sup>1</sup>  
 Anne-Laure Charles,<sup>2</sup> Delphine Duteil,<sup>5</sup> Fabien Alpy,<sup>5</sup> Catherine-Laure Tomasetto,<sup>5</sup>  
Thomas F. Baumert,<sup>1,6,7</sup> and  Joffrey Zoll<sup>2,8,9</sup>

<sup>1</sup>Institute for Translational Medicine and Liver Disease, UMR-S1110, Inserm, University of Strasbourg, Strasbourg, France;

<sup>2</sup>Biomedicine Research Center of Strasbourg (CRBS), UR 3072 “Mitochondrie, Stress oxydant et Plasticité musculaire,”

University of Strasbourg, Strasbourg, France; <sup>3</sup>Faculty of Sport Sciences, University of Strasbourg, Strasbourg, France;

<sup>4</sup>Institute of Cancerology Strasbourg Europe (ICANS), Strasbourg, France; <sup>5</sup>IGBMC UMR 7104-UMR-S 1258, CNRS, Inserm,

Université de Strasbourg, Illkirch, France; <sup>6</sup>IHU Strasbourg, Strasbourg, France; <sup>7</sup>Service d'Hépatogastroentérologie,

University Hospital of Strasbourg, Strasbourg, France; <sup>8</sup>Service de Physiologie et Explorations Fonctionnelles, University

Hospital of Strasbourg, Strasbourg, France; and <sup>9</sup>Faculty of Medicine, University of Strasbourg, Strasbourg, France

## Abstract

Cancer cells rely on glycolysis and lactic fermentation for ATP production, inducing an abnormal glucose uptake in tumors. However, it is largely unknown whether the increased tumor glucose consumption affects overall body glucose homeostasis including perturbation of the liver glucose production pathways. The effect of mammary tumor development on the liver metabolism pathway was examined by using a mouse model based on FVB/N wild-type (WT-SD) and FVB/N-Tg(MMTV-PyVT)634Mul/J mice (Tg-SD), who develop spontaneous mammary tumors. Blood and livers were analyzed for metabolic changes, by measuring histological staining, signaling, and insulin sensitivity. Tg-SD mice developed mammary tumors with an average weight of 6 g, and cancer development increased total food intake without impacting body weight gain. Tumor development did not affect blood glycemia and lactate levels but increased insulin and homeostasis model assessment of insulin resistance (HOMA-IR) index ( $P = 0.06$ ). In the liver, Tg-SD mice with tumors exhibited a decrease in glycogen content and an increase in gluconeogenesis gene expression, as G6pc, Pgc1 $\alpha$ , and Foxo1 ( $P < 0.05$ ), as well as Pepck and Ldha ( $P < 0.01$ ). Moreover, the phosphorylation of AMPK and AKT was significantly decreased ( $P < 0.01$  and  $P < 0.05$ , respectively). Surprisingly, liver fibrosis was markedly increased in Tg mice ( $P < 0.05$ ) alongside elevated inflammatory gene expression, such as IL1 $\beta$  ( $P < 0.01$ ) or IL6 ( $P < 0.05$ ). Here, we found that the development of non-metastatic mammary tumors using the MMTV-PyMT mouse model disrupts liver function through the development of inflammation, fibrosis, and metabolic perturbation, including an increase in glucose production and insulin resistance. Finally, these observations unravel a previously unknown metabolic cross talk between the tumors and the liver.

**NEW & NOTEWORTHY** This work demonstrates that the spontaneous development of non-metastatic mammary tumors triggers hepatic activation of endogenous glucose production pathways, coinciding with the onset of insulin resistance. This finding suggests a significant cross talk between tumors and the liver during tumorigenesis, aiming at enhancing glucose production to meet the elevated energy demands of the tumor. Understanding this interaction could provide insights into metabolic alterations associated with cancer and lead to potential therapeutic targets to inhibit tumor metabolism.

*breast cancer; gluconeogenesis; insulin resistance; liver; Warburg effect*

## INTRODUCTION

Breast cancer is the most commonly diagnosed cancer in women and represents the fourth leading cause of cancer mortality worldwide (1). Compared with healthy cells, cancer cells show specific capabilities that enable tumorigenesis, known as the hallmarks of cancer (2). Of these characteristics,

cancer cells reprogram their energy metabolism and limit the ATP production to glycolysis and lactic fermentation, even in aerobic conditions (3). This ability, defined as the Warburg effect, is greatly in favor of tumorigenesis (4). In addition, given that the lactic fermentation pathway is less efficient than oxidative phosphorylation for ATP production, cancer cells must increase tumor glucose supplies to produce enough



Correspondence: J. Zoll (Joffrey.zoll@unistra.fr).

Submitted 11 December 2024 / Revised 1 February 2025 / Accepted 5 March 2025



energy to growth and proliferate. This is mediated by the increase in glucose receptor and glycolytic enzyme expression (5), resulting in a significant increase in the glycolysis rate (6).

Several studies have suggested that tumors can alter the function of various organs beyond those targeted by metastatic dissemination (7, 8). To date, the liver seems to be a potential peripheral target affected by cancer development, which plays a major role in glucose homeostasis. Indeed, an increase in glucose demand leads to a gluconeogenesis-mediated liver pathway, which uses nonglucose precursors such as pyruvate and lactate, or through the glycogen degradation pathway (9). These pathways involve several enzymes, which are notably regulated by the insulin signaling pathway and the Akt-Foxo1-PGC1 $\alpha$  axis (10). Breast tumor development may trigger hepatic adaptations, where a cross talk could emerge with the tumor to meet its energy demands (8).

However, a detailed understanding of the liver metabolism role in tumorigenesis is largely absent. To address this knowledge gap, we investigated the effects of spontaneous mammary tumor development on peripheral metabolism using a well-established genetic mouse model. Specifically, we focused on liver pathways of endogenous glucose production and the actors involved in their regulation.

## MATERIALS AND METHODS

### Generation of MMTV-PyMT and Mouse Maintenance

Mice were obtained from The Jackson Laboratory. For the generation of MMTV-PyMT female, MMTV-PyMTTg male mice [FVB/N-Tg(MMTV-PyVT)634Mul/J] were crossed with FVB/N-WT female mice. The first generation of females was genotyped for the PyMT transgene by standard PCR using the following PyMT primers: F: 5'-GGAAGCAAGTACTTCACAAGGG-3'; Rev: 5'-GGAAAGTCACTAGGAGCAGGG-3'. All procedures were approved by our local ethics committee (CREMEAS, Strasbourg, agreement numbers: #31118-2021042111176323) and performed following *Guide for the Care and Use of Laboratory Animal Experiments*.

Six-week-old FVB/N-WT (WT-SD,  $n = 7$ ) and FVB/N-Tg(MMTV-PyVT)634Mul/J (Tg-SD,  $n = 8$ ) female mice were maintained by two of three in conventional open-top cages in a temperature-controlled environment at  $\sim 22^{\circ}\text{C}$  under a 12-h light, 12-h dark cycle with ad libitum access to food and water. Mice were fed a standard chow diet (SD), consisting of 20.5% fat, 15.5% protein, and 64% carbohydrates (3.82 kcal/g, Safe Diets) for 8 wk. Design protocol is resumed in Fig. 1A. Shredded paper, cotton sticks, and wood sticks were placed in the cages to reduce animal stress. Weight gain and food intake were weekly measured by electronic balance. At the age of 14-wk-old, the mice were fasted for 4 h and anesthetized through inhalation of 4% isoflurane in a hermetic cage (Aerrane; CSP, Cournon, France). Blood glucose and ketone body levels from the tail vein were measured with a glucose meter (AccuChek Performa; Roche, Basel, Switzerland) and a ketone bodies meter (Freestyle Optium Neo, Abbott, IL). Then, mice were euthanized by cervical dislocation. All mammary tumors and liver were harvested and weighed, and liver samples were snap-frozen in liquid nitrogen for RT-qPCR and Western blot experiments or immersed in 2-methylbutane cooled in liquid nitrogen for histological staining.

Blood was collected into a heparinized tube, and plasma was separated by centrifugation (1,000 g for 10 min at  $4^{\circ}\text{C}$ ) for biochemical analysis. All samples were stored at  $-80^{\circ}\text{C}$ .

### Histological Analysis

After frozen fixation via OCT, liver tissue was sectioned at  $-20^{\circ}\text{C}$  on a cryostat microtome (10  $\mu\text{m}$  thick, Cryostar NX70; Fisher Scientific, MA). For the hematoxylin-eosin and Oil Red O staining, the slides were stained according to the gold standard protocol, as previously described (11). For the periodic acid Schiff staining, cryosections were fixed in Carnoy's fixative for 10 min and stained according to the manufacturer's instructions (395B; Sigma-Aldrich, Missouri). For Masson's trichrome staining, cryosection was fixed in Bouin's fixative solution for 1 h and stained according to the manufacturer's instructions (H15; Sigma-Aldrich, Missouri). All the stained slides were snaped using a Zeiss Apotome.2 microscope (CTK Instruments, California). Positive staining was quantified using Qupath (<https://qupath.github.io>).

### RNA Isolation, Reverse Transcription, and Real-Time Quantitative PCR

Total RNA was extracted from liver with the Kingfisher Duo Prime (Fisher Scientific, Massachusetts) using the MagMAX mirVana Total RNA Isolation Kit according to the manufacturer's instructions. RNA concentration and quality were verified using fluorometric measurement on a Qubit 4 Fluorometer according to the manufacturer's instructions (Invitrogen, California). Procedures of reverse transcription and qPCR amplification were fully described previously (11). Relative gene expression levels were performed in duplicate and normalized to ribosomal phosphoprotein P0 (36b4). Relative gene expression was calculated with the  $\Delta\Delta\text{Ct}$  method. Specific primers are listed in Supplemental Table S1.

### Western Blotting and Antibodies

Procedures of Western blotting were fully described previously (11). Primary antibodies from Cell Signaling were used: anti-total AMPK $\alpha$  (#2532, 1:1,000; Cell Signaling, Massachusetts), anti-phospho AMPK $\alpha$  (Thr172, #2535, 1:1,000; Cell Signaling, Massachusetts), anti-total Akt (#9272, 1:1,000; Cell Signaling, Massachusetts), and anti-phospho AKT (Ser 473, #4060, 1:1,000; Cell Signaling, Massachusetts). Anti-rabbit (1:4,000, No. 7074S; Cell Signaling) or anti-mouse (1:4,000, No. 7076S; Cell Signaling) were used as secondary antibodies. Proteins were revealed using a Pierce ECL kit (Thermo Fisher Scientific, California) or SupraSignal Femto kit (Thermo Fisher Scientific, California) and visualized by enhanced chemiluminescence (iBright 1500 Imaging System; Invitrogen, California). The quantification of protein was performed using ImageJ Software (v. 1.8.0), using the ponceau coloration as the loading control [Romero-Calvo et al. (12)].

### Biochemical Analyses, HOMA-IR, and QUICKI Index

Lactate levels were assayed in duplicate by the colorimetric enzymatic method, according to the manufacturer's instructions (1:50 plasma dilution, MET-5012; Cell Biolabs, Inc., California). Insulin levels were assayed in duplicate by the enzyme-linked immunosorbent assay method, according to the manufacturer's instructions (1:4 plasma dilution,

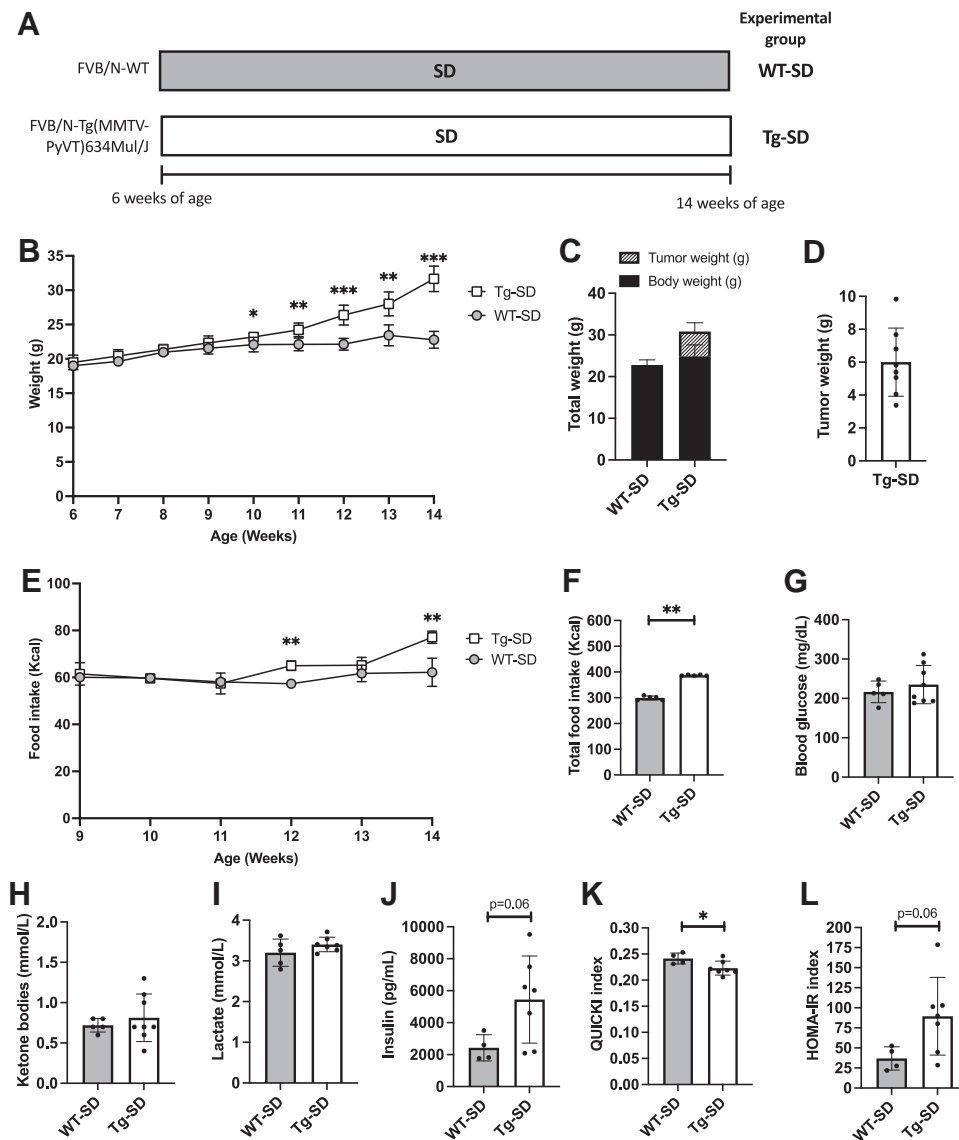


**Figure 1.** Effects of mammary tumor development on weight gain, food intake, and blood parameters. **A:** experimental design of the procedure including wild-type (WT, FVB/N-WT mice) and transgenic group (Tg, FVB/N-Tg(MMTV-PyVT)634Mul/J, fed a standard chow diet for 8 wk. **B:** body weight in grams throughout the procedure ( $n = 7$  or  $8$  mice/group). **C:** details of total weight, with body weight shown in black, and tumor weight for the Tg group shown in hatched lines ( $n = 7$  or  $8$  mice/group). **D:** total tumor weight for the Tg group ( $n = 8$ ). **E:** food intake in kcal throughout the procedure ( $n = 7$  or  $8$  mice/group). **F:** total food intake in kcal ( $n = 7$  or  $8$  mice/group). **G:** fasting blood glucose levels ( $n = 5$  or  $8$  mice/group). **H:** fasting ketone body levels measured from the vein tail after 4 h of fasting. Plasma levels of lactate (**I**) ( $n = 5$  or  $8$  mice/group) and insulin (**J**) ( $n = 4$  or  $8$  mice/group). QUICKI index (**K**) and HOMA-IR index (**L**) ( $n = 4$  or  $8$  mice/group). All data are presented as means  $\pm$  SD, and statistical significance is reported as \* $P < 0.05$ , \*\* $P < 0.01$ , and \*\*\* $P < 0.001$ , Student's  $t$  tests or nonparametric Mann–Whitney. HOMA-IR, homeostasis model assessment of insulin resistance; QUICKI, quantitative insulin sensitivity check index.

EM0260, FineTest; Biotech Co., Ltd., Wuhan, PR China). Insulin resistance was assessed by using the quantitative insulin sensitivity check index (QUICKI) ( $1/\log$  fasting plasma insulin +  $\log$  fasting plasma glucose) and the homeostasis model assessment of insulin resistance (HOMA-IR) index (fasting plasma glucose  $\times$  fasting plasma insulin/22.5).

### Statistical Analysis

Statistical analyses were performed using GraphPad 8 Prism GraphPad Software, Inc. Normal distribution was checked using the Shapiro–Wilk test. Depending on the results, parametric statistical Student's  $t$  tests or non-parametric Mann–Whitney  $U$  tests were used to study the difference between groups.

## RESULTS

### Spontaneous Mammary Tumor Development Increases Total Food Intake and Decreases Insulin Sensitivity

We documented a weight variation throughout the procedure (Fig. 1B). Although WT-SD and Tg-SD mice exhibited

similar weight gain initially, Tg-SD mice showed a significant increase from 10 to 14 wk, reaching +39% compared with WT-SD ( $P < 0.001$ ). To account for tumor growth, we adjusted the final body weight of Tg-SD mice by subtracting the total tumor weight at 14 wk (Fig. 1C). Following this adjustment, Tg-SD mice had a final weight comparable to WT-SD ( $24.8 \pm 2.8$  g vs.  $22.8 \pm 1.2$  g), with tumors accounting for  $6 \pm 2.1$  g of the weight (Fig. 1D).

We measured the effect of mammary tumor development on caloric intake by monitoring food intake between the 9th and 14th weeks of age. In comparison with WT-SD mice, Tg-SD mice showed a significant increase in food intake at 12 wk (+13%,  $P < 0.01$ ) and 14 wk (+24%,  $P < 0.01$ ), leading to a total increase in 88.2 kcal (29%,  $P < 0.01$ ) over the procedure (Fig. 1, E and F).

Blood analysis showed no significant differences in glucose, ketone bodies, or lactate levels between Tg-SD and WT-SD groups (Fig. 1, G–I). However, insulin levels tended to increase in Tg mice (+124%,  $P = 0.063$ , Fig. 1J). Compared with the WT-SD group, the QUICKI index of the Tg-SD was



significantly decreased ( $-8\%$ ,  $P < 0.05$ ), indicating reduced insulin sensitivity (Fig. 1K), whereas the HOMA-IR index tended to increase ( $+142\%$ ,  $P = 0.068$ , Fig. 1L), suggesting the development of insulin resistance.

### Spontaneous Mammary Tumor Development Increases Total Food Intake and Decreases Insulin Sensitivity

We next explored the endogenous glucose production pathways of the liver throughout histological and molecular analyses. First, we found a significant decrease in the glycogen content in the Tg-SD mice in comparison with the WT-SD group ( $-62\%$ ,  $P < 0.01$ , Fig. 2, A and B), suggesting an activation of the glycogen breakdown.

Regarding the relative expression of genes involved in endogenous glucose production (Fig. 2C), Tg-SD mice exhibited a significant increase in *Pepck* ( $+115\%$ ,  $P < 0.01$ ) and *G6pc* ( $+224\%$ ,  $P < 0.05$ ), *Ldh* ( $+123\%$ ,  $P < 0.01$ ) and an increasing trend *Mct1* ( $+45\%$ ,  $P = 0.054$ ), which are all involved in gluconeogenesis. We found not only an increase in *Pygl* ( $+141\%$ ,  $P < 0.05$ ), which is the main enzyme of glycogen breakdown but also an increase in *Gys2* ( $+113\%$ ,  $P < 0.01$ ), involved in glycogen synthesis (Fig. 2D).

Finally, regarding the transcription factors involved in the regulation of hepatic gluconeogenesis (Fig. 2E), Tg-SD mice increased the relative gene expression of *Pgc1 $\alpha$*  ( $+77\%$ ,  $P < 0.05$ ) and *Foxo1* ( $+72\%$ ,  $P < 0.05$ ), in comparison with WT-SD mice. Moreover, Tg-SD mice exhibited a significant decrease in p-AMPK/AMPK and p-AKT/AKT (respectively,  $-79\%$ ,  $P < 0.01$  and  $-59\%$ ,  $P < 0.05$ , Fig. 2, F and G).

### Spontaneous Mammary Tumor Development Increases Total Food Intake and Decreases Insulin Sensitivity

Mice in the Tg-SD group showed a significant increase in liver weight in comparison with the WT group ( $+60\%$ ,  $P < 0.01$ , Fig. 3A). However, hematoxylin-eosin staining did not reveal an increase in steatosis in the Tg-SD group (Fig. 3B), as well as Oil Red O staining ( $-46\%$ ,  $P < 0.01$ , Fig. 3, C and D), suggesting that the increase in liver weight is not due to fat accumulation but may be due to inflammation and fibrosis. Indeed, we observe multiple inflammatory infiltrates in the livers of Tg-SD mice, contrary to the livers of WT-SD mice (Fig. 3B). Regarding inflammatory and fibrosis markers (Fig. 3E), Tg-SD mice exhibited a significant increase in *Il6* ( $+136\%$ ,  $P < 0.05$ ), *Il1 $\beta$*  ( $+202\%$ ,  $P < 0.01$ ), *Tgf $\beta$*  ( $+197\%$ ,  $P < 0.001$ ), *Colla1* ( $+112\%$ ,  $P < 0.05$ ), and *Col3a1* ( $+367\%$ ,  $P < 0.01$ ) gene expression, suggesting the increase in inflammation as well as fibrosis, in comparison with WT-SD mice. Masson's trichrome staining confirmed the significant increase in fibrosis in Tg-SD mice in comparison with the WT-SD group ( $+125\%$ ,  $P < 0.05$ , Fig. 3, F and G).

## DISCUSSION

Here, we found that the development of non-metastatic mammary tumors using the MMTV-PyMT mouse model disrupts liver function, which is characterized by metabolic perturbation including an increase in glucose production and inflammation, and a decrease in insulin signaling.

First, mammary tumor development increased the food consumption, resulting in a 5% increase in the total food

intake, without modifying weight gain. This increase occurs along with tumor growth and strengthens a hallmark of cancer characterized by an increase in energy requirement due to tumor development (13). In patients, it has been estimated that depending on the tumor burden, the additional energy cost linked to the tumor metabolism can reach 190–470 kcal/tumor kg/day, leading to a subsequent significant impact on the total daily energy expenditure (14). Consequently, the high energy demands of cancer cells could not only increase overall energy expenditure but also disrupt the metabolism of liver, a peripheral organ responsible for maintaining glucose homeostasis.

Investigating glucose endogenous pathways, we found that the MMTV-PyMT mice exhibited several hepatic adaptations, as we documented a large upregulation of gluconeogenesis and glycogen breakdown enzymes, suggesting an increased capacity in glucose production. First, in MMTV-PyMT mice, we observed an increase in liver gene expression of *Pepck*, *G6pc*, and *Ldh* and an increased trend in *Mct1*, which suggests an activation of gluconeogenesis (15). Second, the MMTV-PyMT mice also showed a significant decrease in the hepatic glycogen content along with an increase in the *Pygl* gene expression as well as the *Gys2*, showing an activation of the glycogen turnover (16). The simultaneous increase of both glycogenolysis and glycogen synthesis enzymes is a classic mechanism in response to metabolic stress, allowing rapid changes in glucose flux (17). Collectively, our results extend the study of Cao et al. (8), who observed similar hepatic adaptations in a xenograft breast cancer model, suggesting that cancer development enhances hepatic glucose production by converting noncarbohydrate substrates, such as pyruvate and lactate, as well as glycogen, through increased gluconeogenesis and glycogen turnover. Compared with the xenograft model (8), our approach uses a fully immunocompetent genetic model, which better reflects the pathological processes observed in patients and allows for the study of the impact of immune-mediated mechanisms.

The increase in gluconeogenesis in MMTV-PyMT animals could be explained by the impairment of insulin signalization observed in our study. Indeed, under physiological conditions, insulin binding to its receptors leads to the activation of Akt that phosphorylated downstream targets, including FOXO1 (18). When phosphorylated by AKT, FOXO1, and PGC1 $\alpha$  cannot translocate to the nucleus, resulting in a suppression of *Pepck* and *G6pc* expression (19). In our study, MMTV-PyMT mice exhibited an increasing trend in insulin levels and the HOMA-IR index, and the QUICKI index was decreased. In the liver, the AKT phosphorylation was reduced, whereas Foxo1 and Pgc1 $\alpha$  gene expressions were increased, showing a decrease in insulin signaling (20). Moreover, we observed a significant decrease in AMPK activation in MMTV-PyMT mice, whereas AMPK activation is known to participate in decreased gluconeogenesis (21). Interestingly, the association of decreased AMPK activity and insulin resistance has already been described previously (22).

It might correspond to a metabolic adaptive mechanism in response to the stress induced by an energy deficit associated with the tumor's demands (23). Energetic stress can indeed lead to tissue inflammation, which may disrupt the insulin signaling pathway, alter AMPK signaling, and contribute to fibrosis (24, 25). However, despite evidence suggesting systemic

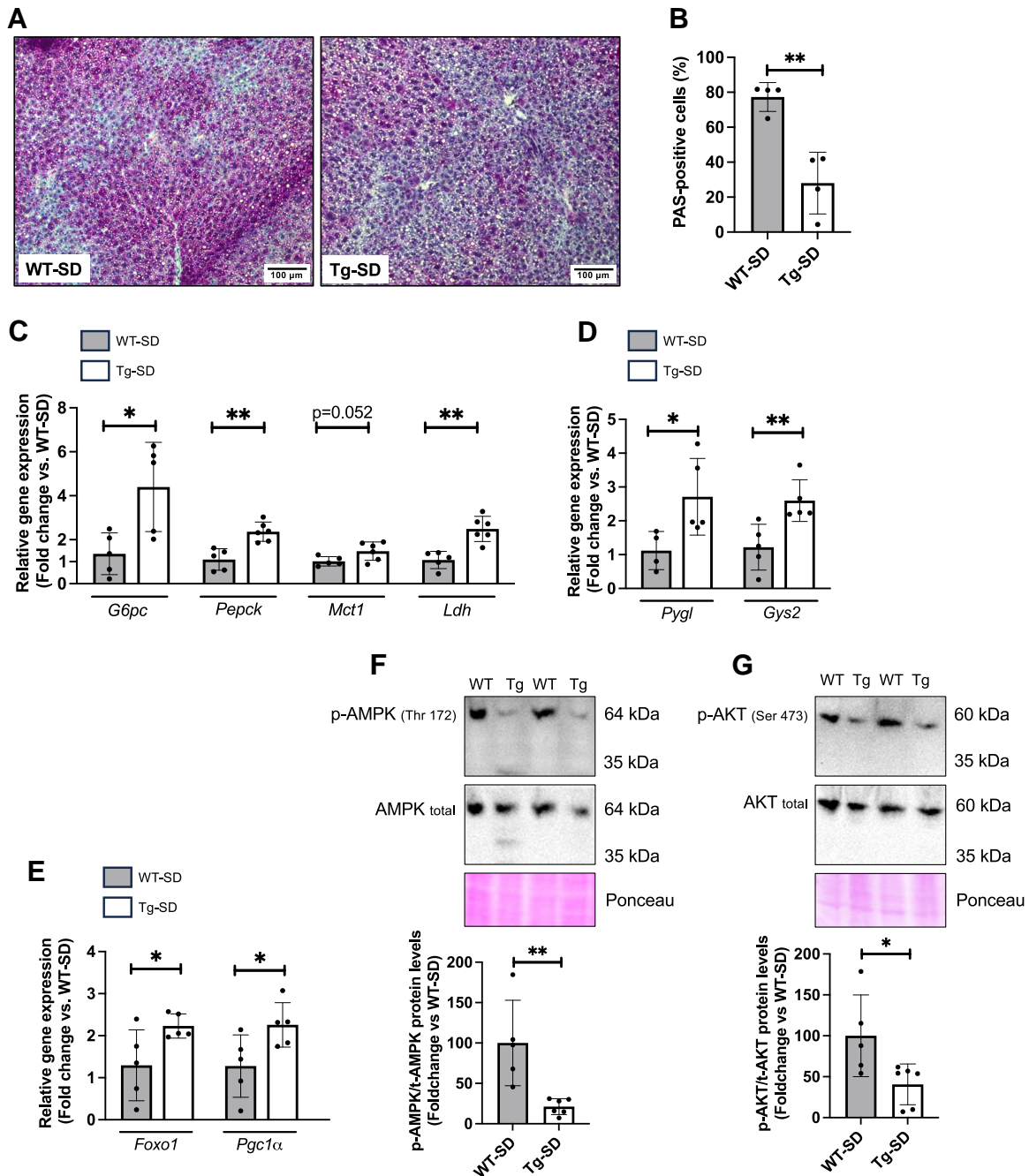


**Figure 2.** Effects of mammary tumor development on glucose metabolism in the liver. **A:** glycogen staining of liver sections. Positive-glycogen cells are stained in purple and negative-glycogen cells are stained in blue. **B:** relative glycogen staining quantification. Relative gene expression of endogenous glucose production (glucose-6 phosphatase catalytic subunit, *G6pc*; phosphoenol pyruvate kinase, *Pepck*; monocarboxylate transporter 1, *Mct1*; lactate dehydrogenase, *Ldh*; **C:** glycogen metabolism (glycogen phosphorylase, *Pygl*; glycogen synthase, *Gys2*; **D:** transcription factors of gluconeogenesis (peroxisome proliferator-activated receptor gamma coactivator 1-alpha, *Pgc1α*; forkhead box O1, *Foxo1*; **E:** Ratio of phosphorylated and total AMP-activated protein kinase protein levels (AMPK; **F:** and protein kinase B (AKT; **G:**). All data are presented as means  $\pm$  SD,  $n = 4$  to 6 mice/group) and statistical significance is reported as \* $P < 0.05$  and \*\* $P < 0.01$ , Student's *t* tests or nonparametric Mann–Whitney.

insulin resistance in our study, our analysis relies a small cohort, on indirect indices (i.e., QUICKI and HOMA-IR) and does not fully capture the dynamics of glucose metabolism and insulin action in the whole organism. Tumors are known to exhibit hyperactivated insulin signaling pathways to enhance glucose uptake and proliferation (26). Therefore, a more detailed investigation of insulin signaling in individual

organs (i.e., liver, kidney, and tumor), with higher effectiveness, is necessary to unravel the potential cross talk between the tumor and peripheral organs.

To better understand glucose fluxes between the liver and the tumor, future studies should explore the expression of glycolytic and gluconeogenic genes in both tissues. In addition, investigating the effects of inhibiting hepatic



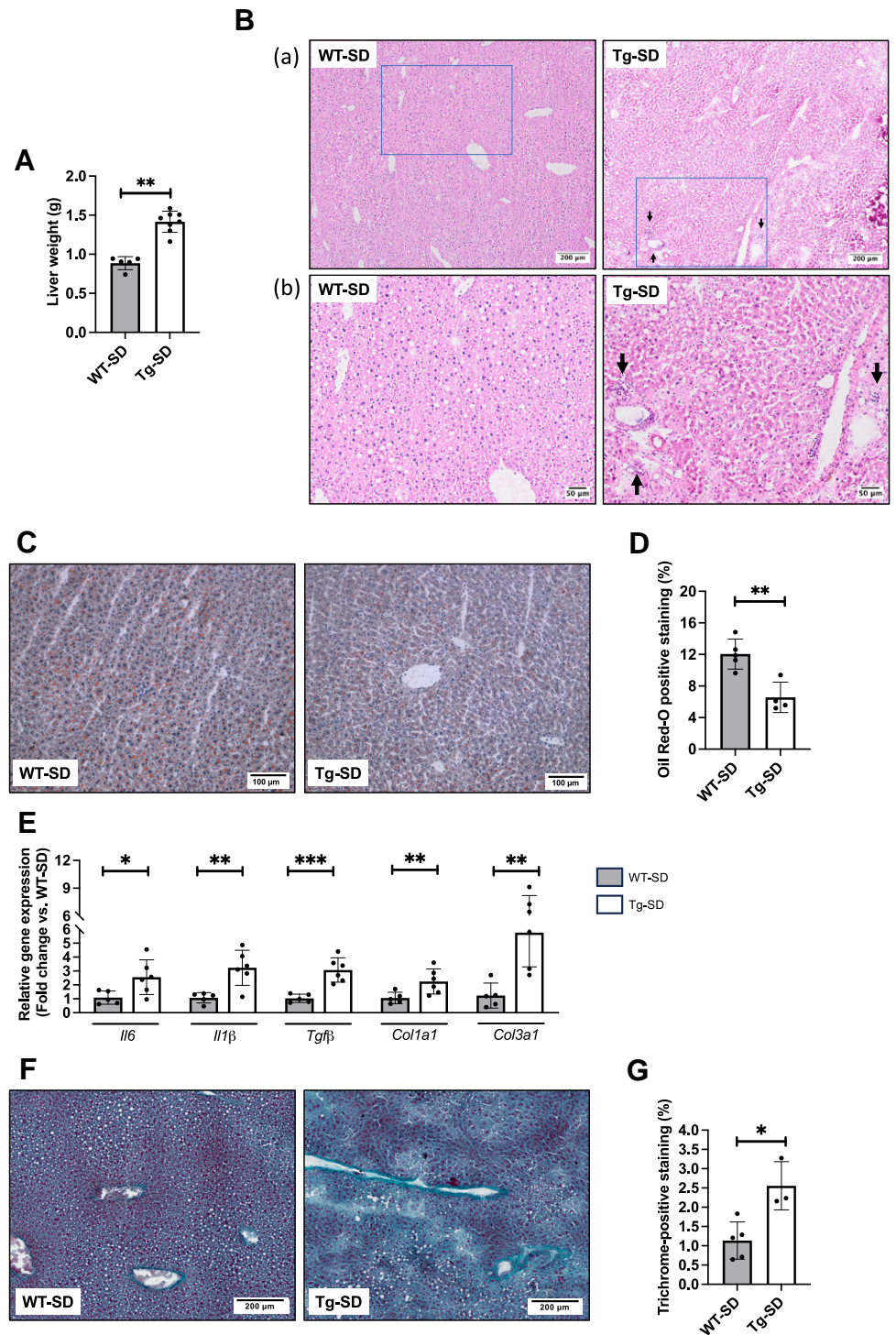


**Figure 3.** Effects of mammary tumor development on hepatic inflammation and fibrosis. **A:** liver weight in grams ( $n = 5$  or  $8$  mice/group). **B:** hematoxylin and eosin staining of liver sections (**a**) with a focus on inflammatory infiltrates (black arrows; **b**). Oil Red O staining of liver sections (**C**) and positive staining quantification (**D**) ( $n = 4$  mice/group). **E:** relative gene expression of interleukin 6, *Il6*; interleukin 1 beta, *Il1β*; transforming growth factor beta, *Tgfβ*; type I collagen, *Col1a1* and type III collagen, *Col3a1* ( $n = 5$  or  $6$  mice/group). Masson's trichrome staining of liver sections (**F**) and positive staining quantification (**G**) ( $n = 3$  or  $5$  mice/group). Images from representative subjects are displayed. All data are presented as means  $\pm$  SD, and statistical significance is reported as  $*P < 0.05$ ,  $**P < 0.01$ , and  $***P < 0.001$ , Student's *t* tests or non-parametric Mann–Whitney.

gluconeogenesis on tumor growth would strengthen this hypothesis. Currently, numerous studies focus on the use of metformin, an antidiabetic drug that improves insulin sensitivity and reduces gluconeogenesis, as a potential adjuvant in cancer treatment (27). Although the effects of metformin remain debated, they highlight the relevance of targeting liver metabolism to reduce tumor growth. Accordingly, our findings suggest that future research should assess the impact of gluconeogenesis inhibitors,

such as metformin or other modulators, in combination with standard cancer treatments.

## Conclusions

This study demonstrates that the spontaneous development of mammary tumors leads to hepatic activation of endogenous glucose production pathways, following the impairment of insulin signaling. Moreover, the metabolic perturbations were associated with liver inflammation and

fibrosis. Our results suggest that a cross talk between the tumors and the liver occurs during tumor development, aimed at increasing endogenous glucose production to meet the elevated energy demands of the tumor. Additional studies are needed to understand the mechanisms underlying the cross talk between the liver and the tumors, as well as the clinical implications of the observed hepatic metabolic perturbations in patients.

## DATA AVAILABILITY

Data will be made available upon reasonable request.

## SUPPLEMENTAL MATERIAL

Supplemental Table S1: <https://www.doi.org/10.6084/m9.figshare.28553306>.

## ACKNOWLEDGMENTS

We thank Marine Oudot and Sarah Durand (Inserm U1110, University of Strasbourg) for the help with histological staining, Julien Friant for the help with the qPCR, and Isabelle Georg for the help with daily care and maintenance of the mice.

## GRANTS

Research of the J.Z. team is supported in part by funding from the association “Alsace Contre le Cancer” and the University of Strasbourg.

## DISCLOSURES

No conflicts of interest, financial or otherwise, are declared by the authors.

## AUTHOR CONTRIBUTIONS

A.C., F.A., C.-L.T., and J.Z. conceived and designed research; A.C., A.B., and J.M. performed experiments; A.C., A.B., and J.M. analyzed data; A.C., A.B., J.M., A.J., E.C., A.-L.C., D.D., F.A., C.-L.T., and T.F.B. interpreted results of experiments; A.C. prepared figures; A.C. and J.Z. drafted manuscript; A.C., A.B., J.M., A.J., E.C., A.-L.C., D.D., F.A., C.-L.T., T.F.B., and J.Z. edited and revised manuscript; A.C., A.B., J.M., A.J., E.C., A.-L.C., D.D., F.A., C.-L.T., T.F.B., and J.Z. approved final version of manuscript.

## REFERENCES

1. Bray F, Laversanne M, Sung H, Ferlay J, Siegel RL, Soerjomataram I, Jemal A. Global cancer statistics 2022: GLOBOCAN estimates of incidence and mortality worldwide for 36 cancers in 185 countries. *CA Cancer J Clin* 74: 229–263, 2024. doi:10.3322/caac.21834.
2. Hanahan D, Weinberg RA. Hallmarks of cancer: the next generation. *Cell* 144: 646–674, 2011. doi:10.1016/j.cell.2011.02.013.
3. Warburg O. On the origin of cancer cells. *Science* 123: 309–314, 1956. doi:10.1126/science.123.3191.309.
4. San-Millán I, Brooks GA. Reexamining cancer metabolism: lactate production for carcinogenesis could be the purpose and explanation of the Warburg Effect. *Carcinogenesis* 38: 119–133, 2017. doi:10.1093/carcin/bgw127.
5. Lin X, Xiao Z, Chen T, Liang SH, Guo H. Glucose metabolism on tumor plasticity, diagnosis, and treatment. *Front Oncol* 10: 317, 2020. doi:10.3389/fonc.2020.00317.
6. Bulmuş Tüccar T, Acar Tek N. Determining the factors affecting energy metabolism and energy requirement in cancer patients. *J Res Med Sci* 26: 124, 2021. doi:10.4103/jrms.JRMS\_844\_20.
7. Wang G, Li J, Bojmar L, Chen H, Li Z, Tobias GC, et al. Tumour extracellular vesicles and particles induce liver metabolic dysfunction. *Nature* 618: 374–382, 2023. doi:10.1038/s41586-023-06114-4.
8. Cao M, Isaac R, Yan W, Ruan X, Jiang L, Wan Y, Wang J, Wang E, Caron C, Neben S, Drygin D, Pizzo DP, Wu X, Liu X, Chin AR, Fong MY, Gao Z, Guo K, Fadare O, Schwab RB, Yuan Y, Yost SE, Mortimer J, Zhong W, Ying W, Bui JD, Sears DD, Olefsky JM, Wang SE. Cancer-cell-secreted extracellular vesicles suppress insulin secretion through miR-122 to impair systemic glucose homeostasis and contribute to tumour growth. *Nat Cell Biol* 24: 954–967, 2022. doi:10.1038/s41556-022-00919-7.
9. Adeva-Andany MM, Pérez-Felpete N, Fernández-Fernández C, Donapetry-García C, Pazos-García C. Liver glucose metabolism in humans. *Biosci Rep* 36: e00416, 2016. doi:10.1042/bsr20160385.
10. Puigserver P, Rhee J, Donovan J, Walkey CJ, Yoon JC, Oriente F, Kitamura Y, Altomonte J, Dong H, Accili D, Spiegelman BM. Insulin-regulated hepatic gluconeogenesis through FOXO1–PGC-1 $\alpha$  interaction. *Nature* 423: 550–555, 2003. doi:10.1038/nature01667.
11. Charlot A, Bringolf A, Debrut L, Mallard J, Charles A-L, Crouchet E, Duteil D, Geny B, Zoll J. Changes in macronutrients during dieting lead to weight cycling and metabolic complications in mouse model. *Nutrients* 16: 646, 2024. doi:10.3390/nu16050646.
12. Romero-Calvo I, Ocón B, Martínez-Moya P, Suárez MD, Zarzuelo A, Martínez-Augustín O, De Medina FS. Reversible Ponceau staining as a loading control alternative to actin in Western blots. *Anal Biochem* 401: 318–320, 2010. doi:10.1016/j.ab.2010.02.036.
13. Thomas F, Rome S, Mery F, Dawson E, Montagne J, Biro PA, Beckmann C, Renaud F, Poulin R, Raymond M, Ujvari B. Changes in diet associated with cancer: An evolutionary perspective. *Evol Appl* 10: 651–657, 2017. doi:10.1111/eva.12465.
14. Friesen DE, Baracos VE, Tuszyński JA. Modeling the energetic cost of cancer as a result of altered energy metabolism: implications for cachexia. *Theor Biol Model* 12: 17, 2015. doi:10.1186/s12976-015-0015-0.
15. Petersen MC, Vatner DF, Shulman GI. Regulation of hepatic glucose metabolism in health and disease. *Nat Rev Endocrinol* 13: 572–587, 2017. doi:10.1038/nrendo.2017.80.
16. Agius L. Role of glycogen phosphorylase in liver glycogen metabolism. *Mol Aspects Med* 46: 34–45, 2015. doi:10.1016/j.mam.2015.09.002.
17. Gonzalez JT, Fuchs CJ, Betts JA, Van Loon LJC. Liver glycogen metabolism during and after prolonged endurance-type exercise. *Am J Physiol Endocrinol Physiol* 311: E543–E553, 2016. doi:10.1152/ajpendo.00232.2016.
18. Biggs WH 3rd, Meisenhelder J, Hunter T, Cavenee WK, Arden KC. Protein kinase B/Akt-mediated phosphorylation promotes nuclear exclusion of the winged helix transcription factor FKHR1. *Proc Natl Acad Sci USA* 96: 7421–7426, 1999. doi:10.1073/pnas.96.13.7421.
19. He L, Li Y, Zeng N, Stiles BL. Regulation of basal expression of hepatic PECK and G6Pase by AKT2. *Biochem J* 477: 1021–1031, 2020. doi:10.1042/BCJ20190570.
20. Sattiel AR. Insulin signaling in health and disease. *J Clin Invest* 131: e142241, 2021. doi:10.1172/JCI142241.
21. Foretz M, Ancellin N, Andreelli F, Saintillan Y, Grondin P, Kahn A, Thorens B, Vaulont S, Viollet B. Short-term overexpression of a constitutively active form of AMP-activated protein kinase in the liver leads to mild hypoglycemia and fatty liver. *Diabetes* 54: 1331–1339, 2005. doi:10.2337/diabetes.54.5.1331.
22. Ruderman NB, Carling D, Prentki M, Cacicedo JM. AMPK, insulin resistance, and the metabolic syndrome. *J Clin Invest* 123: 2764–2772, 2013. doi:10.1172/JCI67227.
23. Tsatsoulis A, Mantzaris MD, Bellou S, Andrikoula M. Insulin resistance: an adaptive mechanism becomes maladaptive in the current environment—an evolutionary perspective. *Metabolism* 62: 622–633, 2013. doi:10.1016/j.metabol.2012.11.004.
24. Fève B, Bastard J-P. The role of interleukins in insulin resistance and type 2 diabetes mellitus. *Nat Rev Endocrinol* 5: 305–311, 2009. doi:10.1038/nrendo.2009.62.
25. Liu K, Yang L, Wang G, Liu J, Zhao X, Wang Y, Li J, Yang J. Metabolic stress drives sympathetic neuropathy within the liver. *Cell Metab* 33: 666–675.e4, 2021. doi:10.1016/j.cmet.2021.01.012.
26. Poloz Y, Stambolic V. Obesity and cancer, a case for insulin signaling. *Cell Death Dis* 6: e2037–e2037, 2015. doi:10.1038/cddis.2015.381.
27. Coyle C, Cafferty FH, Vale C, Langley RE. Metformin as an adjuvant treatment for cancer: a systematic review and meta-analysis. *Ann Oncol* 27: 2184–2195, 2016. doi:10.1093/annonc/mdw410.